Saumen Datta[1]
Manjappara V. Uma[2]
N. Shamala[1]
P. Balaram[2]
[1] *Department of Physics, Indian Institute of Science, Bangalore 560012, India*

[2] *Molecular Biophysics Unit, India Institute of Science, Bangalor 560012, India*

Stereochemistry of Schellman Motifs in Peptides: Crystal Structure of a Hexapeptide with a C-Terminus 6 → 1 Hydrogen Bond

Abstract: *The Schellman motif is a widely observed helix terminating structural motif in proteins, which is generated when the C-terminus residue adopts a left-handed helical (α_L) conformation. The resulting hydrogen-bonding pattern involves the formation of an intramolecular 6 → 1 interaction. This helix terminating motif is readily mimicked in synthetic helical peptides by placing an achiral residue at the penultimate position of the sequence. Thus far, the Schellman motif has been characterized crystallographically only in peptide helices of length 7 residues or greater. The structure of the hexapeptide Boc–Pro–Aib–Gly–Leu–Aib–Leu–OMe in crystals reveal a short helical stretch terminated by a Schellman motif, with the formation of 6 → 1 C-terminus hydrogen bond. The crystals are in the space group $P2_12_12_1$ with* a = *18.155(3) Å,* b = *18.864(8) Å,* c = *11.834(4) Å, and* Z = *4 . The final* R_1 *and* wR_2 *values are 7.68 and 14.6%, respectively , for 1524 observed reflections [*$F_o \geq 3\sigma(F_o)$*]. A 6 → 1 hydrogen bond between Pro(1)CO · · · Leu(6)NH and a 5 → 2 hydrogen bond between Aib(2)CO · · · Aib(5)NH are observed. An analysis of the available oligopeptides having an achiral Aib residue at the penultimate position suggests that chain length and sequence effects may be the other determining factors in formation of Schellman motifs.*

Keywords: *stereochemistry; Schellman motifs; peptides; crystal structure; hexapeptide*

INTRODUCTION

Helical structures in polypeptides are characterized by several contiguous residues in the polymer chain adopting backbone dihedral angles in a limited region of conformational space.[1,2] In the case of right-handed α-helices the characteristic Ramachandran angles are $\phi \approx -57°$, $\psi, \approx -47°$[3] Helix termination is then achieved by residues at the N- and C-termini adopting nonhelical conformations. Major regions of allowed conformational space for helix terminating L-amino acid residues lie in the extended ($\phi \approx -120°$, $\psi \approx 120°$) and semiextended ($\phi \approx -60°$, $\psi \approx 120°$) region of the Ramachandran map.[4] An especially important class of terminating residue conformations was recognized by Charlotte Schellman,[5]

Correspondence to: P. Balaram; email: pb@mbu.iisc.ernet.in
Contract grant sponsor: Department of Science and Technology, Government of India

who noted that helices in proteins were frequently terminated by the C-terminus residue adopting left-handed helical (α_L) conformations ($\phi \approx 60°$, $\psi \approx 30°$). This stereochemical feature, where helix termination occurs by chiral reversal of ϕ,ψ values, is widely observed in protein crystal structures[6–9] and has been termed the Schellman motif .[7] The terminating residue is invariably an achiral amino acid Gly and to a much lesser extent Asn, which has a relatively high propensity for α_L-conformations.[10]

In synthetic peptides, Schellman motifs have been widely characterized in crystal structures of peptide helices containing achiral residues, almost invariably α-aminoisobutyric acid (Aib), at the penultimate position at the C-terminus.[11] In principle the Schellman motif can be formed by a succession of residues with the conformational motif α_R–α_R–α_R–α_L and could therefore be observed even in a protected tetrapeptide that has hydrogen-bonding CO and NH functions in the terminal protecting groups (e.g., Boc and NHMe at the N- and C-terminus, respectively). Thus far, the Schellman motif has been characterized crystallographically only in peptide helices of length 7 residues or greater.

We describe below the crystal structure of a synthetic hexapeptide Boc–Pro–Aib–Gly–Leu–Aib–Leu–OMe, related to the C-terminal segment of the peptide antibiotic efrapeptin[12,13] in which a short helical segment is terminated by chiral reversal. The structure also reveals an interesting hydration pattern, which is of relevance in the context of recent discussions on the role of hydrated peptide backbones in the folding process.[14,15]

EXPERIMENTAL PROCEDURE

Crystallization and X-Ray Diffraction Data Collection

The peptide Boc–Pro–Aib–Gly–Leu–Aib–Leu–OMe (**1**) was synthesized by conventional solution phase procedures, and purified by medium pressure liquid chromatography on a 40–60μ, C_{18} column using methanol–water gradients for elution. Crystals of the peptide **1** were grown from a methanol/water solution by slow evaporation. The x-ray diffraction data were collected from dry crystals of peptide **1** on an automated four circle diffractometer. Unit cell parameters were obtained and refined by least squares fit of the angular settings of 25 accurately determined reflections in the range of $0° < \theta < 25°$. Three-dimensional MoK_α ($\lambda = 0.7107$ Å) intensity data were collected upto $2\theta = 54°$. An ω-2θ scan with variable scan speed was used. Three reflections, monitored after every 15 minutes of x-ray exposure, showed less than 3% variation in intensities. Lorentz polarization corrections were applied, but not the absorption corrections [μ(**1**) = 0.08 mm^{-1}]. All the parameters relevant to the data collection are listed in Table I.

Table I Data Collection and Refinement Parameters for Peptide 1

Empirical formula	$C_{33}O_9N_6H_{57}$
Crystal habit	Clear rectangular
Crystal size (mm)	0.4 × 0.2 × 0.1
Crystallizing solvent	CH_3OH/H_2O
Space group	$P2_12_12_1$
Cell parameters	
a (Å)	18.155(5)
b (Å)	18.864(8)
c (Å)	11.834(4)
Volume (Å^3)	4052.9
Z	4
Molecules/asym. unit	1
Cocrystallized solvent	None
Molecular weight	698.8
Density (g/cm) (calc)	1.145
F(000)	1512
Radiation (Å)	MoK_α ($\lambda = 0.7107$)
2θ Range (°)	50
Scan type	$\omega - 2\theta$
Scan speed	Variable
Independent reflections	2987
Observed reflections. [$\|F\| > 3\ \sigma(F)$]	1524
Goodness-of-fit (*S*)	1.18
$\Delta\rho_{max}$ (eÅ^{-3})	0.18
$\Delta\rho_{min}$ (eÅ^{-3})	−0.25
Final *R*	7.68%
Final R_W	14.6%
Data-to-parameter ratio	3 : 1

Structure Solution and Refinement

The crystal structure of **1** was determined by the vector search method[16] followed by partial structure expansion.[17] Patterson maps were computed using SHELX-86.[18] The computer program PATSEE[16] was used for proper orientation and translation of the fragment used as the model in the vector or Patterson search. Partial structure expansion was done using SHELX-86.

The approach of using direct methods was not successful in yielding the structure. Subsequent attempts using the vector search methods with models of different helical conformations or Schellman motif modules were unsuccessful. The use of the backbone [CO(Aib)–Pro–Ala–NH(Aib)] of the underlined segment of the sequence Boc–Trp–Ile–Ala–Aib–Ile–Val–Aib–Leu–<u>Aib</u>–<u>Pro</u>–<u>Ala</u>–<u>Aib</u>–Pro–Aib–Pro–Phe–OMe[19] as a model fragment was successful in determining the structure. A sharpened Patterson map and 250 largest $|E|$ values were used in the vector search method. Proper orientation and translation were identified

on the basis of highest rotational figure of merit (RFOM) and highest combined figure of merit (CFOM).[16]

The fragment containing 14 atoms was then used in the partial structure expansion method employing 250 reflections satisfying the criterion $E_{obs} > 1.5$ and the largest values of E_{calc}/E_{obs}. The Fourier map generated revealed 45 atoms out of 48 nonhydrogen atoms in the asymmetric unit. The remaining nonhydrogen atoms were located from the difference Fourier map.

A full-matrix least-squares refinement was carried out using SHELX-93.[20] All the nonhydrogen atoms were initially refined isotropically. The hydrogen atoms were fixed geometrically in the idealized positions with C—H = 1.08 Å and N—H = 1.08 Å, and refined in the final cycle of refinement as riding over the atoms they are bonded. The final R factor was 0.0768 (R_w = 0.146) for 1524 observed reflections, with $F_o \geq 3\sigma(F_o)$. The function minimized during refinement was $\Sigma w(|F_o \text{ minus; } F|)^2$, where $w = 1/[\sigma^2 \times (Fo^2) + (.0910 \times P)^2]$, where $P = [\text{Max } (Fo^2, 0) + 2(Fc^2)]/3$. The crystallographic coordinates (nonhydrogen and hydrogen atoms) and thermal parameters of peptide **1** are being deposited in the Cambridge Crystallographic Data File and are also available on request from authors.*

Table II Torsion Angles[a] (deg) in Peptide 1

Residue	ϕ	Ψ	ω	χ^1	χ^2
Pro(1)[e]	−54[b]	−42	−175		
Aib(2)	−57	−43	−177		
Gly(3)	−74	−16	178		
Leu(4)	−100	6	180	−69	168, −69
Aib(5)	60	42	178		
Leu(6)	−113	166[c]	167[d]	−58	169, −69

[a] The definition of torsion angles for rotation about bonds of the peptide backbone (ϕ, φ, and ω) and about bonds of the amino acid side chains (χ^1, χ^2) are as suggested by the IUPAC-IUB Commission on Biochemical Nomenclature (1970).[30] Estimated standard deviations ~ 1.0°.

[b] C′(0)—N(1)—C$^\alpha$(1)—C′(1).

[c] N(6)—C$^\alpha$(6)—C′(6)—O(OMe).

[d] C$^\alpha$(6)—C′(6)—O(OMe)—C(OMe).

[e] The pyrrolidine ring torsion angles for Pro(1) are (χ^n, degrees) χ^1(N—C$^\alpha$—C$^\beta$—C$^\gamma$) = −24, χ^2(C$^\alpha$—C$^\beta$—C$^\gamma$—C$^\delta$) = 29, χ^3(C$^\beta$—C$^\gamma$—C$^\delta$—N) = −22, χ^4(C$^\gamma$—C$^\delta$—N—C$^\alpha$) = 7, and θ(C$^\delta$—N—C$^\alpha$—C$^\beta$) = 10.

RESULTS AND DISCUSSION

Crystal State Conformation of Peptide 1

Torsion angles and the comparative 4 → 1/5 → 1 hydrogen-bond parameters for Boc–Pro–Aib–Gly–Leu–Aib–Leu–OMe are listed in Table II and Table III, respectively. Figure 1 shows the stereo view of the molecular conformation in crystals. Backbone dihedral angles indicate that the first three residues Pro(1), Aib(2), and Gly(3) form a right-handed helical turn, whereas Leu(4) and Aib(5) residues fall in the bridge region and the left-handed helical regions of the Ramachandran plot (Table III). Inspection of the parameters for potential 4 → 1 and 5 → 1 interactions suggest that the molecule possesses three relatively weak 4 → 1 hydrogen bonds CO(0) · · · NH(3), CO(1) · · · NH(4), and CO(2) · · · NH(5). While the CO(0) · · · NH(4) and CO(1) · · · NH(5) distances are comparable to the distances normally observed for 4 → 1 hydrogen bonds, the O · · · H distances are significantly longer. Although all the intramolecular hydrogen-bonding interactions observed in the helical turn are relatively weak, the helix terminating 6 → 1 hydrogen bond formed between CO(1) · · · NH(6) is characterized by much shorter N · · · O (3.02 Å) and O · · · H (2.18 Å) distances. The Schellman motif is formed by the chiral reversal at Aib(5) and backbone distortions at Leu(4) leading to both 6 → 1 (C_{16}) and 5 → 2 (C_{10}) interactions. This feature has been identified as a "paper clip" in protein structures by Milner-White.[7] The 4 → 1 hydrogen bond encased within the Schellman motif module appears to represent a relatively weak interaction as suggested by the longer N · · · O (3.41 Å) and H · · · O (2.59 Å) distances, a feature that has also been noted earlier.[11]

Side-Chain Conformations

Both Leu side chains assume $g^-(tg^-)$ conformations. Although, the most widespread leucine side-chain conformations in peptides as well as in proteins are $g^-(tg^-)$ and $t(g^+t)$, the former is most prevalent.[21–23] The pyrrolidine ring torsional angles for Pro(1) (Table II, footnote e) establish a C$^\gamma$-*exo* puckering for the five-membered ring.[24]

Packing

Figure 2 shows the molecular packing in crystals. All the symmetry-related molecules in the unit cell are held together by weak van der Waals interactions. Molecules are arranged *head-to-tail* in the crystal along the *c* axis, with a bridging water molecule inserted between translationally related peptides (Figure 2). Hydrogen bonds are formed involving the water molecule, which are bifurcated in nature

* Supplementary material consisting of coordinates (nonhydrogen and hydrogen atoms), bond lengths, bond angles, and thermal parameters will be deposited with the Cambridge Structural Data Base, University Chemical Laboratory, Lensfield Road, Cambridge CB21EW, UK. Observed and calculated structure factors can be obtained on request.

Table III Parameters for Potential Hydrogen Bonds in the Structure 1

			N···O	H···O	C═O···H	C═O···N	O···HN
Type	Donor	Acceptor	Distance (Å)			Angle (deg)	
Intramolecular							
4 → 1[b]	N(3)	O(0)	3.14	2.53	115	125	129
4 → 1[b]	N(4)	O(1)	3.06	2.35	102	112	141
4 → 1[b]	N(5)	O(2)	3.41	2.59	103	105	161
4 → 1	N(6)	O(3)	6.43	5.86	44	50	128
5 → 1	N(4)	O(0)	3.38	2.74	143	154	132
5 → 1	N(5)	O(1)	3.22	2.89	149	163	105
5 → 1	N(6)	O(2)	4.87	4.18	84	91	140
6 → 1[b]	N(6)	O(1)	3.02	2.18	147	144	167

Intermolecular	Donor	Acceptor	Distance (Å)	Angle (deg)
[b]	N(2)[a]	W	2.99 [N(2)[a]···W]	172[N(2)[a]···H(2)···W]
[b]	W	O(4)	3.00 [W···O(4)]	149 [C′(4)···O(4)···W]
[b]	W	O(5)	2.93 [W···O(5)]	107 [C′(5)···O(5)···W]

[a] Symmetrically related by the relation (x, y, $z - 1$).
[b] Acceptable hydrogen bonds.[31–33]

[NH(2) · · · W · · · CO(4) and NH(2) · · · W · · · CO(5)] (Table III). Helical peptides in crystals have almost always been observed to pack in head-to-tail motifs that result in long rods or columns of helices throughout the crystal.[25,26] In crystals, where the succeeding α- and 3_{10}-helices in a column are in good register

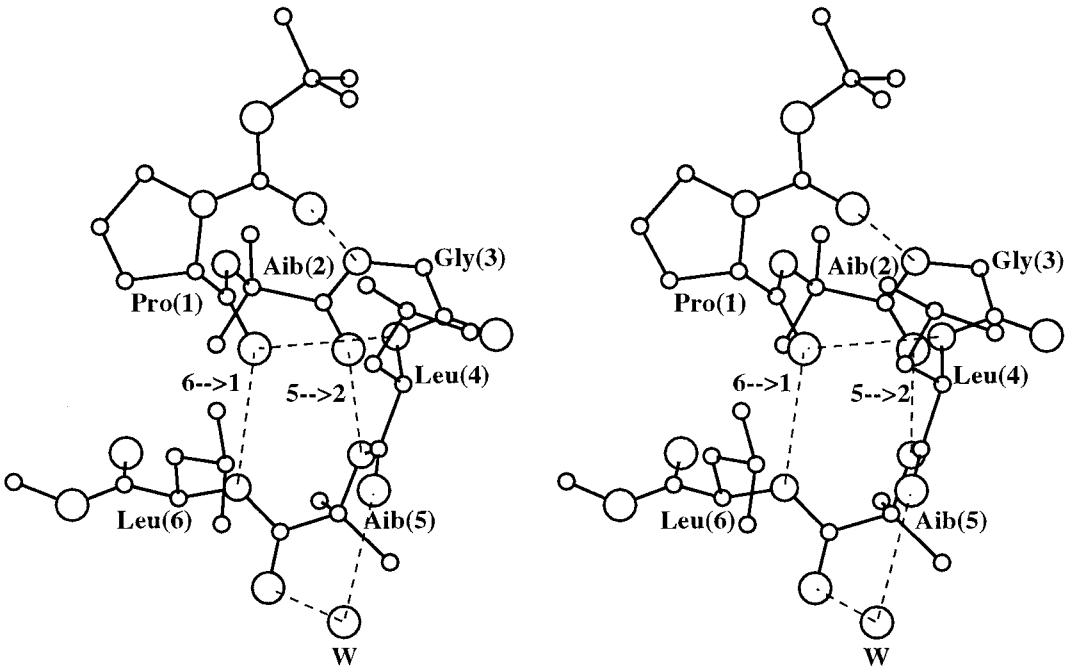

FIGURE 1 Stereo view of peptide **1** in crystals. Intramolecular hydrogen bonds are indicated by broken lines.

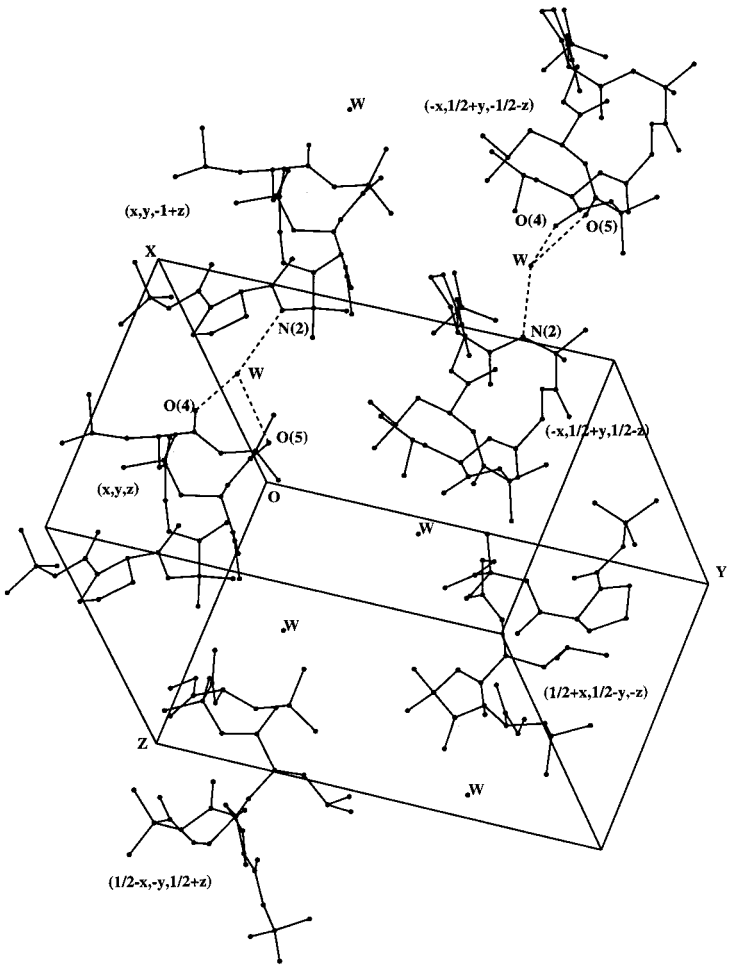

FIGURE 2 Packing diagram for peptide **1** in crystals. Intermolecular hydrogen bonds are indicated by broken lines.

with respect to each other, 3 and 2 intermolecular NH · · · CO hydrogen bonds, respectively, can be formed between the head of one helix and the tail of another. In some crystals where the ends of the succeeding helices are not in good register, only 1 intermolecular NH · · · CO hydrogen bond may form, expanded by water or alcohol molecules that mediate the hydrogen bonds.[27,28] Despite being in perfect register in crystals, the helices of peptide **1** were unable to form the two intermolecular head-to-tail hydrogen bonds due to the reversal of helical sense at the C-terminus as well as the absence of the NH group in the N-terminus.

Hydration

The structure of **1** reveals a water molecule that is simultaneously hydrogen bonded to both Leu(4) and Aib(5) CO groups. The relative orientation of the two CO groups is determined by the ϕ,ψ torsion angles at Aib(5), which is in fact the site of chiral reversal. The ability of water molecules to orient hydrogen-bonding groups in peptides has been suggested to be important as a mechanism for the formation of short-range nucleation sites in protein folding.[14] Transient hydrated structures have recently been invoked in order to rationalize rapid conformational fluctuations in heteropolypeptides.[15] Crystal structures of peptides frequently provide a static view of specific modes of hydration.

Schellman Motif in Short Peptides

The observation of 6 $\rightarrow$ 1 (C_{16}) hydrogen-bonded structures formed by chiral reversal at an achiral residue, either Aib or ΔPhe (α,β-dehydrophenylalanine) in synthetic peptide helices is a relatively common feature. Table IV summarizes torsion angles for res-

Table IV Torsion Angles at C-Terminus Residues in Helical Oligopeptides Having a Terminating 6 → 1 Hydrogen Bond

	T − 3		T − 2		T − 1		T[a]		T − 1	
	ϕ	Ψ	ϕ	Ψ	ϕ	Ψ	ϕ	Ψ	ϕ	Ψ
Sequence[b]	(deg)		(deg)		(deg)		(deg)		(deg)	
Peptide I	−78	−37	−59	−31	−100	9	74	18	−107	31
Peptide II	−77	−38	−56	−36	−88	−4	60	44	55	43
Peptide IIIa	−79	−40	−53	−37	−83	−5	64	33	−113	37
Peptide IIIb	−59	−30	−59	−30	−114	12	52	48	−102	−11
Peptide IV	−65	−29	−70	−25	−108	13	67	36	−115	144
Peptide V	−63	−35	−70	−20	−106	17	65	35	−126	167
Peptide VI	−57	−43	−74	−16	−100	6	60	42	−113	166
Peptide VII	−77	−9	−93	14	−124	19	65	33	82	
Peptide VIII	−64	−23	−61	−30	−98	15	84	10	−114	
Peptide IX	−72	−39	−57	−33	−96	16	68	31	−57	151
Peptide X	−72	−36	−58	−28	−92	7	65	28	−114	22
Peptide XI[c]	−65	−23	−64	−24	−81	−16	53	49	−59	−39
Peptide XII	−68	−48	−55	−36	−78	−21	56	46	−57	146
Peptide XIII	−75	−40	−63	−23	−84	−10	96	−4	−63	−39
Peptide XIV	−68	−35	−54	−35	−91	10	62	39	−137	−171
Peptide XV[c]	78	34	62	31	74	19	−63	−26	−60	−36
Peptide XVI[c]	−54	−49	−78	−9	−80	−18	56	32	85	−3
Peptide XVII	[d]		−86	−18	49	48	−53	−41		

[a] T represents the helix terminating residue that is the site of chiral reversal. The residue preceding and following T are sequentially numbered.

[b] Sequences of peptides and references in parentheses:
Peptide I: Boc–Val–Aib–Phe–Aib–Ala–Aib–Leu–OMe (Ref. 34).
Peptide II: Boc–Val–Aib–Leu–Aib–Ala–Aib–Phe–OMe (Ref. 34).
Peptide III: Boc–Val–Aib–Leu–Aib–Ala–Aib–Leu–OMe (Ref. 34).
Peptide IV: Boc–Leu–Aib–Val–Ala–Leu–Aib–Val–OMe (Ref. 35).
Peptide V: Boc–Leu–Aib–Val–Gly–Leu–Aib–Val–OMe (Ref. 11).
Peptide VI: Boc–Pro–Aib–Gly–Leu–Aib–Leu–OMe (this study).
Peptide VII: Ac–ΔPhe–Val–ΔPhe–Phe–Ala–Val–ΔPhe–Gly–OMe (Ref. 36).
Peptide VIII: Boc–Val–ΔPhe–Phe–Ala–Leu–Ala–ΔPhe–Leu–OH (Ref. 37).
Peptide IX: pBrBz–$(Aib–Ala)_5$–OMe · $2H_2O$ (from aqueous methanol solution; Ref. 38).
Peptide X: pBrBz–$(Aib–Ala)_6$–OMe · $2H_2O$ (Ref. 38).
Peptide XI: Boc–Leu–Aib–Val–Gly–Gly–Leu–Aib–Val–OMe (Ref. 39).
Peptide XII: Boc–$(Ala–Aib)_2$–Ala–Glu(OBzl)–$(Ala–Aib)_2$–Ala–OMe (Ref. 40).
Peptide XIII: Boc–Val–ΔPhe–Leu–Phe–Ala–ΔPhe–Leu–OMe (Ref. 41).
Peptide XIV: pBrBz–$(Aib–Ala)_5$–OMe (from a DMSO–isopropanol solvent mixture; Ref. 42).
Peptide XV: Boc–D(Val–Ala–Leu–Aib–Val–Ala–Leu)–L(Val–Ala–Leu–Aib–Val–Ala–Leu)–OMe (Ref. 43).
Peptide XVI: Boc–Gly–Dpg–Gly–Gly–Dpg–Gly–NHMe (Ref. 44); Dpg: α,α-di-n-propylglycine).
Peptide XVII: Boc–Leu–Aib–Val–β–Ala–γ–Abu–Leu–Aib–Val–OMe (Ref. 45).

[c] The potential 6 → 1 hydrogen bond in this case is solvated. The interaction between CO(3) and NH(8) groups in peptide XI is mediated by the OH group of a methanol molecule. Solvent insertion (methanol) is also observed between CO(4) and NH(9) groups in peptide XV and between CO(1) and NH(6) groups in peptide XVI.

[d] The definition of the backbone dihedral angles of the residues β-Ala ($\phi = -130°$, $\theta = 76°$, $\Psi = -162°$) and γ-Abu ($\phi = -108°$, $\theta_1 = 58°$, $\theta_2 = 66°$, $\Psi = -169°$) are as suggested by Banerjee and Balaram (Ref. 46).

idues encompassing the Schellman motif and the C-terminal flanking residue in available crystal structures. The terminating residue (T) is defined as the residue that adopts the α_L conformation and signals helix termination. It is clear that the ϕ,ψ values at the penultimate residue (T-1) drift into the bridge region of the Ramachandran map, with considerable variation in the torsion angles. The terminating residue (T) conformations are more closely clustered into left-handed helical (α_L) regions. In principle, in all these cases the Aib/ΔPhe residues could have adopted right-handed helical (α_R) conformations, which would have

Table V Torsion Angles in Oligopeptides Lacking a 6 → 1 Hydrogen Bond, Possessing an Achiral Residue at the Penultimate Position

	T − 5		T − 4		T − 3		T − 2		T − 1		T[a]		T + 1	
	ϕ	Ψ	ϕ	Ψ	ϕ	Ψ	ϕ	Ψ	ϕ	Ψ	ϕ	Ψ	ϕ	Ψ
Sequence[b]	(deg)		(deg)		(deg)		(deg)		(deg)		(deg)		(deg)	
Peptide I	−55	−47	−66	−38	−61	−44	−59	−36	−73	−28	50	51	−62	144
Peptide II	−55	−48	−70	−28	−68	−48	−57	−42	−69	−28	51	53	−65	−14
Peptide III	−59	−37	−76	−45	−59	−36	−58	−28	−81	−17	46	50	−70	168
Peptide IV	−56	−47	−65	−42	−64	−41	−59	−38	−72	−32	51	52	−62	147
Peptide V	−63	−17	−56	−21	−55	−23	−50	−32	−57	−36	−71	−23	−80	156
Peptide VI	−68	−16	−60	−23	−61	−17	−46	−25	−69	−15	−55	−35	154	
Peptide VII			−60	−40	−73	−11	−58	−25	−56	−33	−66	−17	−70	158
Peptide VIII	−57	−34	−56	−43	−67	−36	−53	−52	−65	−44	−65	−16	−84	153
Peptide IX					−51	−46	−74	−11	−106	−52	−61	−37	−104	−56
Peptide X					−56	145	55	34	56	38	60	40	−53	144
Peptide XI														
Molecule A							−57	−39	−76	−9	−102	−59	−64	−34
Molecule B							−55	−35	−61	−20	−97	10	−54	−46
Peptide XII			77	41	−46	−24	−63	−19	−67	−8	−61	−26	−122	26

[a] "T" represents the helix terminating residue which is the site of chiral reversal. The residue preceding and following T are sequentially numbered.

[b] Sequences of peptides and references in parentheses:
Peptide I: Boc–Trp–Ile–Ala–Aib–Ile–Val–Aib–Leu–Aib–Pro–OMe (Ref. 47).
Peptide II: Ac–Trp–Ile–Ala–Aib–Ile–Val–Aib–Leu–Aib–Pro–OMe (Ref. 47).
Peptide III: Boc–Trp–Ile–Ala–Aib–Ile–Val–Aib–Leu–Aib–Pro–OMe (anhydrous; Ref. 48).
Peptide IV: Boc–Trp–Ile–Ala–Aib–Ile–Val–Aib–Leu–Aib–Pro–OMe · $2H_2O$ (Ref. 49).
Peptide V: Boc–Val–Aib–Val–Aib–Val–Aib–Val–OMe (Ref. 50).
Peptide VI: Boc–Val–ΔPhe–Phe–Ala–Phe–ΔPhe–Val–ΔPhe–Gly–OMe (Ref. 51).
Peptide VII: pBrBz–$(Aib–Ala)_3$–OMe (Ref. 52).
Peptide VIII: pBrBz–$(Aib–Ala)_4$–OMe · $2H_2O$ (Ref. 52).
Peptide IX: Boc–Aib–Pro–Val–Aib–Val–OMe (Ref. 53).
Peptide X: pCl–Z–Pro–Aib–Ala–Aib–Ala–OMe (Ref. 54).
Peptide XI: Z–Aib–Ala–Leu–Aib–NHMe (Ref. 55).
Peptide XII: Boc–Phe–ΔPhe–Val–Phe–ΔPhe–Val–OMe (Ref. 56).

resulted in the continuation of the right-handed helix formed by the N-terminal segment. The difference in energies between the continuous right-handed helical conformation and α_L-terminated structures is not expected to be appreciable, since the number of intramolecular hydrogen bonds, in principle, are the same in both the cases. In order to clarify the role of chain length and specific sequence effects, which determine the precise nature of the α_L-terminated conformation of peptide helices, we examined structure of peptides that contain an achiral residue at the penultimate position but do not form intramolecular 6 → 1 hydrogen bonds (Table V). Inspection of Table V reveals that in the case of peptides I– IV chiral reversal is indeed observed at the Aib residue that terminates the helix. However, 6 → 1 hydrogen–bond formation is precluded by the presence of a Pro residue at the C-terminus, which lacks the hydrogen–bonding NH function. This suggests that 6 → 1 hydrogen bonding is not the driving force for the observed chiral reversal. In peptide V to IX the penultimate Aib/ΔPhe residues in the sequence adopt the α_R conformation. Interestingly, in these four examples the preceding residue (T-1) is Val or Ala. Inspection of the seventeen examples in Table IV reveals that the T-1 residue is Leu in 5 cases, Ala in 9 cases, and Val in 1 case. It is possible that the Schellman motif formation or chiral reversal at the penultimate residue in the sequence is facilitated by the intrinsic tendency of the T-1 residue to adopt conformations in the bridge region of the Ramachandran map. In order to estimate the propensities of Leu, Val, and Ala residues for ϕ,ψ distortions in the helical region, we examined the torsion angle distribution of these residues in the body of available crystal structures of peptide helices. Figure 3 illustrates the observed distribution. Although

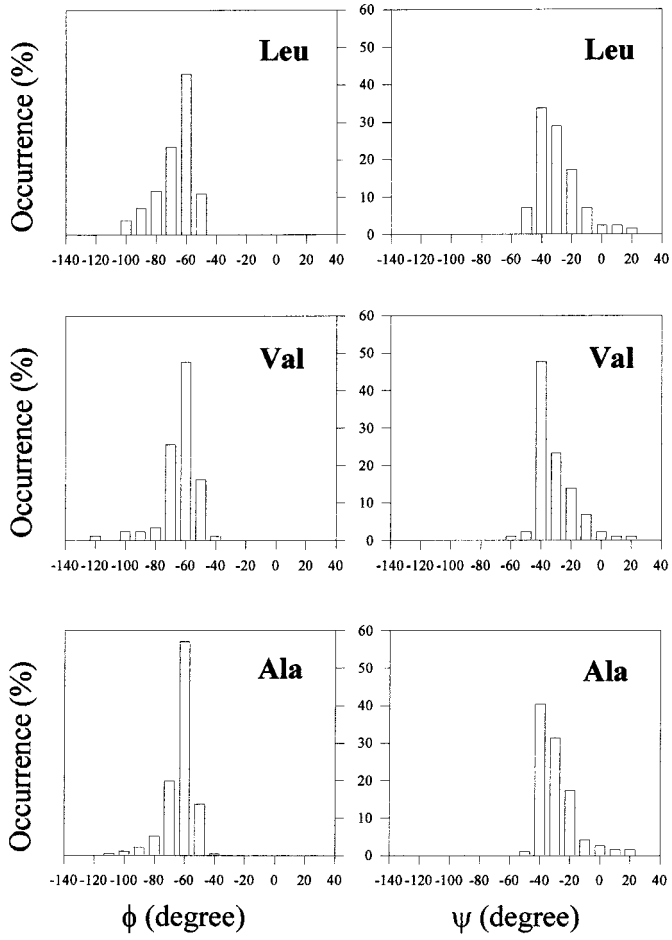

FIGURE 3 Distribution of the dihedral angles ϕ and ψ (in degrees) in residues Leu (top), Val middle), and Ala (bottom) in helical peptides. The histogram interval is 10°. The sample includes 128 Leu, 86 Val,and 191 Ala residues, from the crystal structures of 71 helical peptides. Helix chain length varies from six to sixteen residues.

the observed sample size is relatively small, the tendency of Leu residues to adopt more negative ϕ values and more positive ψ values, corresponding to the bridge region of ϕ,ψ space, is clearly evident.This feature has been noted in an earlier analysis based on fewer structures.[29] The structure of peptide X listed in Table V may be viewed as an exception. Although the penultimate Aib in the sequence adopts an α_L conformation, the preceding residue also adopts an α_L conformation. The structure may be viewed as a distorted type II β-turn followed by two consecutive type III′ β-turns.

The structure of peptide XI (Z–Aib–Ala–Leu–Aib–NHMe) in Table V is an example where despite the appropriate positioning of an Aib residue at the C-terminus, chiral reversal and $6 \rightarrow 1$ hydrogen-bond formation is not observed. In this case the two independent molecules in the crystals adopt conformations thar lie close to 3_{10}- and α-helical structures. Interestingly, in both molecules the Leu residue adopts backbone dihedral angles significantly deviated from the idealized helical values (molecule A: $\phi = -102°$, $\psi = -59°$; molecule B: $\phi = -97°$, $\psi = 10°$). In principle, peptide Z–Aib–Ala–Leu–Aib–NHMe represents the shortest segment in which an idealized Schellman motif could have formed. An analysis of the sequences listed in Table V suggests that multiple factors determine the stereochemistry of the C-terminus in helical peptides. Clearly, energetic differences between the α_R and α_L conformations of an achiral residue placed at the potential helix terminating position in peptides are small. The possible role of crystal packing effects cannot therefore be entirely neglected. The present analysis suggests that local sequences may be important in determining whether or not chiral reversal is observed, when an achiral residue is placed at the penultimate position of a sequence. The precise role of chain length and sequence effects in Schellman

motif formation merits further investigation.

This research was supported by the Department of Science and Technology, Government of India.

REFERENCES

1. Richardson, J. S. Adv Protein Chem 1981, 34, 167–330.
2. Barlow, D. J.; Thornton, J. M. J Mol Biol 1988, 201, 601–619.
3. Creighton, T. E. Proteins: Structure and Molecular Properties, 2nd ed.; W. H. Freeman and company: New York, 1992.
4. Gunasekaran, K.; Nagarajaram, H. A.; Ramakrishnan, C.; Balaram, P. 1998, J Mol Biol 215, 915–930.
5. Schellman, C. In Protein Folding; Jaenicke, R., Ed.; Elsevier/North-Holland: New York, 1980; pp 53–61.
6. Milner-White, E. J. 1988 J. Mol. Biol., 199, 503–511.
7. Aurora, R.; Srinivasan, R.; Rose, G. D. Science 1994, 264, 1126–1130.
8. Nagarajaram, H. A., Sowdhamini, R., Ramakrishanan, C. and Balaram, P.(1993) *FEBS Lett*. **321**, 79–83
9. Rajashankar, K. R. and Ramakumar, S.(1996) *Protein Science*, **5**, 932–946
10. Srinivasan, N, Anuradha, V. S., Ramakrishanan, C., Sowdhamini, R. and Balaram, P. (1994) *Int. J. Peptide Protein Res*., **44**, 112–122
11. Datta, S., Shamala, N., Banerjee, A., Pramanik, A., Bhattacharjya, S. and Balaram, P.(1997) *J. Am. Chem. Soc*., **119**, 9246–9251 (and references therein)
12. Krishna, K.; Sukumar, M.; Balaram, P. Pure Appl Chem 1990, 62, 1417–1420.
13. Gupta, S.; Krasnoff, S. B.; Roberts, D. W.; Renwick, J. A. A.; Brinen, L. S.; Clardy, J. J Org Chem 1992, 57, 2306–2313.
14. Simmerling, C. L.; Elber, R. Proc. Natl. Acad. Sci. USA 1995, 92, 3190–3193.
15. Barron, L. D.; Hecht, L.; Wilson, G. Biochemistry 1997, 36, 13143–13147.
16. Egert, E.; Sheldrick, G. M. Acta Cryst 1985, A41, 262–268.
17. Karle, J. Acta Cryst 1968, B24, 182–186.
18. Sheldrick, G. M. SHELX 86 Program for Crystal Structure Determination; University of Gottingen: Gottingen, Germany, 1986.
19. Karle, I. L.; Flippen-Anderson, J.; Sukumar, M.; Balaram, P. Proc Natl Acad Sci USA 1987, 84, 5087–5091.
20. Sheldrick, G. M. SHELX 93 Program for Crystal Structure Refinement; University of Gottingen: Gottingen, Germany, 1993.
21. Janin, J.; Wodak, S.; Levitt, M.; Maigret, B. J Mol Biol 1978, 125, 357–386.
22. Benedetti, E.; Morelli, G.; Némethy, G.; Scheraga, H. A. Int J Peptide Protein Res 1983, 22, 1–15.
23. Bhat, T. N.; Sasisekharan, V.; Vijayan, M. 1979, Int J Peptide Protein Res 13, 170–184.
24. Ramachandran, G.; Lakshminarayanan, A. V.; Balasubramanian, R.; Tegoni, G. Biochem Biophys Acta 1970, 221, 165–181.
25. Karle, I. L. Acta Crystallogr B 1992, 48, 341–356.
26. Karle, I. L. Biopolymers (Peptide Science) 1996, 40, 157–180.
27. Karle, I. L.; Flippen-Anderson, J. L.; Uma, K.; Balaram, P. 1988, Int J Peptide Protein Res 32, 536–543.
28. Karle, I. L.; Flippen-Anderson, J. L.; Uma, K.; Sukumar, M.; Balaram, P. J Am Chem Soc 1990, 112, 9350–9356.
29. Karle, I. L.; Balaram, P. Biochemistry 1990, 29, 6747–6756.
30. IUPAC-IUB Commission on Biochemical Nomenclature Biochemistry 1970, 9, 3471–3479.
31. Datta, S.; Shamala, N.; Banerjee, A.; Balaram, P. J Peptide Res 1997, 49, 604–611.
32. Baker, E. N.; Hubbard, R. E. Progr Biophys Mol Biol 1984, 44, 97–179.
33. Toniolo, C. CRC Crit. Rev. Biochem 1980, 9, 1–44.
34. Karle, I. L.; Flippen-Anderson, J. L.; Uma, K.; Balaram, P. Int. J. Peptide Protein Res. 1993, 42, 401–410.
35. Banerjee, A.; Datta, S.; Pramanik, A.; Shamala, N.; Balaram, P. 1996, J. Am Chem Soc 118, 9477–9483.
36. Rajashankar, K. R.; Ramakumar, S.; Jain, R. M.; Chauhan, V. S. J. Am Chem Soc 1995, 117, 11773–11779.
37. Rajashankar, K R.; Ramakumar, S.; Jain, R. M.; Chauhan, V. S. 1996, J Biomol Struct Dynam 13, 641–647.
38. Benedetti, E.; Di Blasio, B.; Pavone, V.; Pedone, C.; Santini, A.; Bavoso, A.; Toniolo, C.; Crisma, M.; Sartore, L. J Chem Soc Perkin Trans 1990, 2, 1829–1837.
39. Karle, I. L.; Banerjee, A.;, Bhattacharjya, S.; Balaram, P. Biopolymers 1996,38, 515–526.
40. Bosch, R.; Jung, G.; Schmitt, H.; Winter, W. Biopolymers 1985, 24, 961–978.
41. Rajashankar, K. R.; Ramakumar, S.; Mal, T. K.; Jain, R. M.; Chauhan, V. S. Angew Chem Int Ed Engl 1996, 35, 765–768.
42. Di Blasio, B.; Pavone, V.; Saviano, R.; Fattorusso, C.; Pedone, E.; Benedetti, E.; Crisma, M.; Toniolo, C. Peptide Res 1994, 7, 55–59.
43. Banerjee, A.; Raghothama, S. R.; Karle, I. L.; Balaram, P. Biopolymers 1996,39, 279–285.
44. Karle, I. L.; Kaul, R.; Balaji Rao, R.; Raghothama, S.; Balaram, P. J Am Chem Soc 1997, 119, 12048–12054.
45. Karle, I. L.; Pramanik, A.; Banerjee, A.; Bhattacharjya, S.; Balaram, P. J Am Chem Soc 1997, 119, 9087–9095.
46. Banerjee, A.; Balaram, P. Curr Sci 1997, 73, 1067–1077.

47. Karle, I. L.; Flippen-Anderson, J. .L.; Sukumar, M.; Balaram, P. Int J Peptide Protein Res 1990, 35, 518–526.
48. Karle, I. L.; Flippen-Anderson, J. L.; Sukumar, M.; Balaram, P. Int J Peptide Protein Res 1988, 31, 567–576.
49. Karle, I. L.; Flippen-Anderson, J. .L.; Sukumar, M.; Balaram, P. Proc Natl Acad Sci USA 1986, 83, 9284–9288.
50. Francis, A. K.; Vijaykumar, E. K. S.; Balaram, P.; Vijayan, M. 1985, Int J Peptide Protein Res 1986, 26, 214–223.
51. Rajashankar, K. R.; Ramakumar, S.; Chauhan,V. S. J Am Chem Soc 1992, 114, 9225–9226.
52. Pavone, C.; Benedetti, E.; Di Blasio, B.; Pedone, C.; Santini, A.; Bavoso, A.; Toniolo, C.; Crisma, M.; Sartore, L. J Biomol Struct Dynam 1990, 7, 1321–1331.
53. Francis, A. K.; Iqbal, M.; Balaram, P.; Vijayan, M. J Chem Soc Perkin Trans 1982, 2, 1235–1239.
54. Cameron, T. S.; Hanson, A. W.;Taylor, A. Cryst Struct Commun 1982, 11, 321–330.
55. Benedetti, R.; Di Blasio, B.; Galdiero, S.; Pedone, C.; Saviano, M.; Moretto, V.; Crisma, M.; Toniolo, C. Gazz Chim Ital 1996, 126, 569–575.
56. Padmanabhan, B.; Singh, T. P. Biopolymers, 1993, 33, 613–619.